Mineralogical and geochemical studies of ironstones around Koton karfi, part of southern Bida Basin, north central Nigeria

JOHN UZOMA MEGWARA[1,*], SOLOMON IOKOSO ABA'A [2] , IDRIS ISA FUNTUA [3]

[1]Applied and Engineering Geology Department, Nigerian Geological Survey Agency, Kaduna, Nigeria

[2] Geology Department, Federal University of Technology, Lafia, Nigeria

[3] Umar Musa Yar'adua University, Katsina, Nigeria.

ABSTRACT

The combination of mineralogical and geochemical data of sedimentary rocks can reveal the nature of rocks and the tectonic settings of the sedimentary basin. Ironstone deposits cap plateaux around Koton Karfi requiring detailed studies. The survey area is bounded by longitudes 6˚48′00″ E to 6˚52′48″ E and latitudes 8˚05′00″ N to 8˚10′46″ N covering an area of about 96.8 km^2. The stratigraphic successions in the study area consist of the basal Lokoja Formation, overlain by the Patti Formation and capped by the Agbaja Formation. The basal Lokoja Formation is a sequence of matrix supported conglomerates and sandstones overlying the Pre–Cambrian Basement. Twenty one rock samples were collected from the study area. Geochemical analysis of the samples was carried out using x-ray fluorescence. Mineralogical analysis determined the mineral compositions and modal percentages of minerals in the samples. Twenty elements and nineteen oxides were revealed and they include Al_2O_3, SiO_2, Fe_2O_3, P_2O_5, CaO, K_2O, V_2O_5, Cr_2O_3, Eu_2O_3, NiO_2, ZnO, La_2O_3, BaO, SrO, CuO, Nd_2O_3, Re_2O_7 and PbO. The mineralogical study shows the presence of two petrographic varieties namely the ooidal pack-ironstone and detrital mud-ironstone. The core of the ooids is made up of pseudomorphs of goethite after siderite and hematite after Itabirite.

KEY WORDS Framboid, Goethite, Hematite, Itabirite, Magnetite.

1.0 INTRODUCTION

Ironstone is a sedimentary rock, either deposited directly as a ferruginous sediment or formed by chemical replacement that contains a substantial proportion of an iron (Fe) compound from which iron can be smelted commercially. The iron minerals comprising ironstones can consist either of oxides: limonite, hematite and magnetite; carbonates: siderite; silicates: chamosite; or some combination of these minerals. Iron exists naturally in ironstone (sometimes called iron ore). Iron ores are rocks and minerals from which metallic iron can be economically extracted (Chard, 1995).

The significance attached to the growth of the steel sector has led to interest in the ironstone deposits of Nigeria. Two broad types of iron deposits occur prominently in Nigeria. They are: (i) Banded Iron Formation (BIF): The Formation occurs in folded bands and lenses associated with the Pre-Cambrian metasedimentary schist belts outcropping in the western half of the country. The iron formation bands which vary in thickness from about 3 cm to 5 m are found commonly in groups intercalated within surrounding country rocks or as isolated thin units. The bands have variable strike extent with some stretching though discontinuously for several kilometers.

Prominent locations include Tajimi, Itapke, Ajabanoko, Ochokochoko Toto, Farin Ruwa, Birnin Gwari, Maru, Jamare, Kaura Namoda, Kakun, Isanlu, Roni and Ogbomosho areas (MSMD, 2010). (ii) The Cretaceous sedimentary (oolitic) iron deposits: Although they are described as sedimentary, they are partly lateritic in character and occur prominently around Agbaja, Koton Karfi and Nsudde areas in the north central and south eastern zones of the country respectively (MSMD, 2010). According to Obaje (2009), Koton Karfi hosts prominent ironstone bodies requiring detailed investigation. The ironstone deposits cap hills and table lands around Koton Karfi.

Tattam (1943), suggested that the sediments outcropping at the south–eastern end of the Bida Basin (Figure 1), are laterally continuous with beds in the Anambra Basin occurring at the stratigraphical level of the Enugu Shale and Adeleye (1973) regarded the Patti Formation and Lokoja Sandstone as the lateral equivalents of the Mamu Formation and Enugu Shales respectively. Adeleye (1973) correlated the Batati/Agbaja ironstones with the Dukamaje Formation in the Sokoto Basin, concluding that the Bida Basin was affected by a Maastrichtian transgression advancing from the northwest.

Adeleye (1973) and Oresajo (1979) suggested a synsedimentary origin for the ironstones because their depositional characteristics and relationship with other sediments of the Bida Basin show that the ooids were formed within a high energy domain. The lateritic model was first postulated due to the absence of fossils in the ironstone beds (Du Preez, 1956), and to the presence of iron oxide and hydroxide in the ooids (Jones, 1955, 1958; Kogbe, 1978).

Ladipo *et al*. (1988, 1993); Mucke (1993) and Mucke *et al*. (1994) suggested a post–diagenetic iron enrichment for the ironstone deposits. This survey thus focuses on the mineralization of ironstone in the study area due to recent specialized industrial demands for the ore. Various analyses will reveal the mineralization pattern of the ore. This is achieved by carrying out intensive geochemical and petrographic studies of the ironstone samples.

1.1 Location and Accessibility

The study area is located along the Abuja-Lokoja road, around Koton Karfi, southern Bida Basin; with longitude 6°48′00″ E to 6°52′48″ E and latitude 8°05′00″ N to 8°10′46″ N, covering an area of 96.8 km^2 and accessible through footpaths as shown in Figure 2.

Two distinct climatic conditions mark the survey area; which are the annual wet and dry season periods. The wet season influenced by the tropical maritime winds, is experienced during the months of March to October, with mean annual rainfall of 1560 mm. The dry season is influenced by the northeasterly Harmattan winds which prevail between the months of November to February. Humidity during this period ranges from about 30% to 35% and the area is usually characterized by dusty haze (Oguntoyinbo, 1978). After the departure of the Harmattan and in the absence of rain, the hot sunny season with temperatures exceeding 27°C sets in. The mean annual temperature of the area is 20°C (Balogun, 2000). The study area falls within the woodland savannah vegetation belt (Abimbola, 1994). Typified by high grass, shrubs and low trees. Within the study area, vegetation changes with season, in the wet season it flourishes while in the dry season much of it withers and dies. Along the stream courses where the soil is wet, thicker vegetation called fringing forest is found (Oguntoyinbo, 1978).

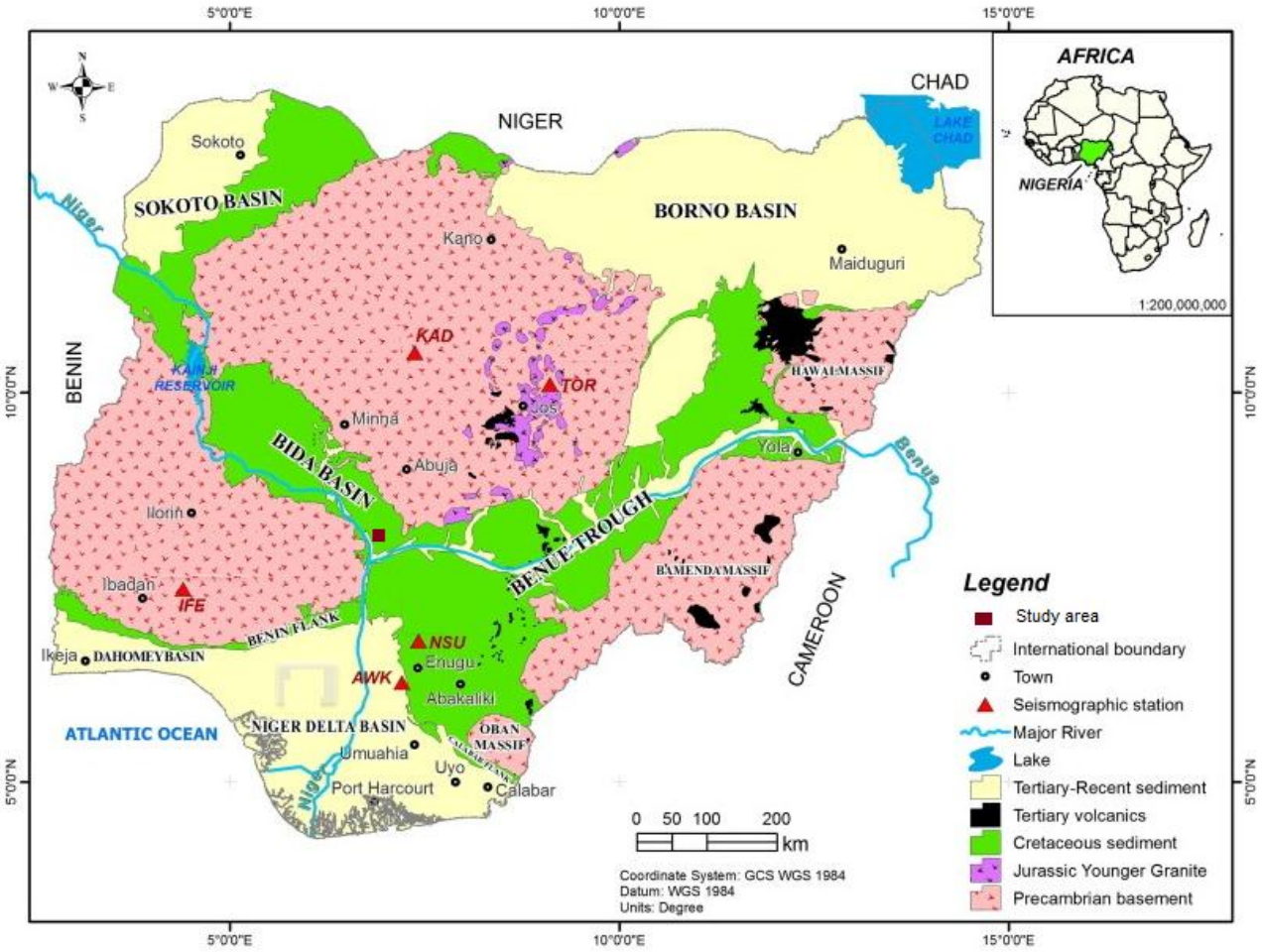

Fig.1 Geological map of Nigeria showing the Bida Basin (Adapted: Akpan *et al.*, 2016)

The survey area is characterized by irregular ridges, steep hills and table lands. Elevation ranges from about 200 m to 300 m. The table lands are capped by laterites which support little vegetation. Edges of the hills form sharp escarpment with occasional break in slope, indicative of the influence of erosion and presence of resistant indurated sandstone beds. The area is drained by the flood plain of river Niger marked by elongated ponds and streams (Oguntoyinbo, 1978). Flow pattern is in the habit of branching tree roots, such that tributaries branch out from streams in different directions; mostly at acute angles, (Figure 2).

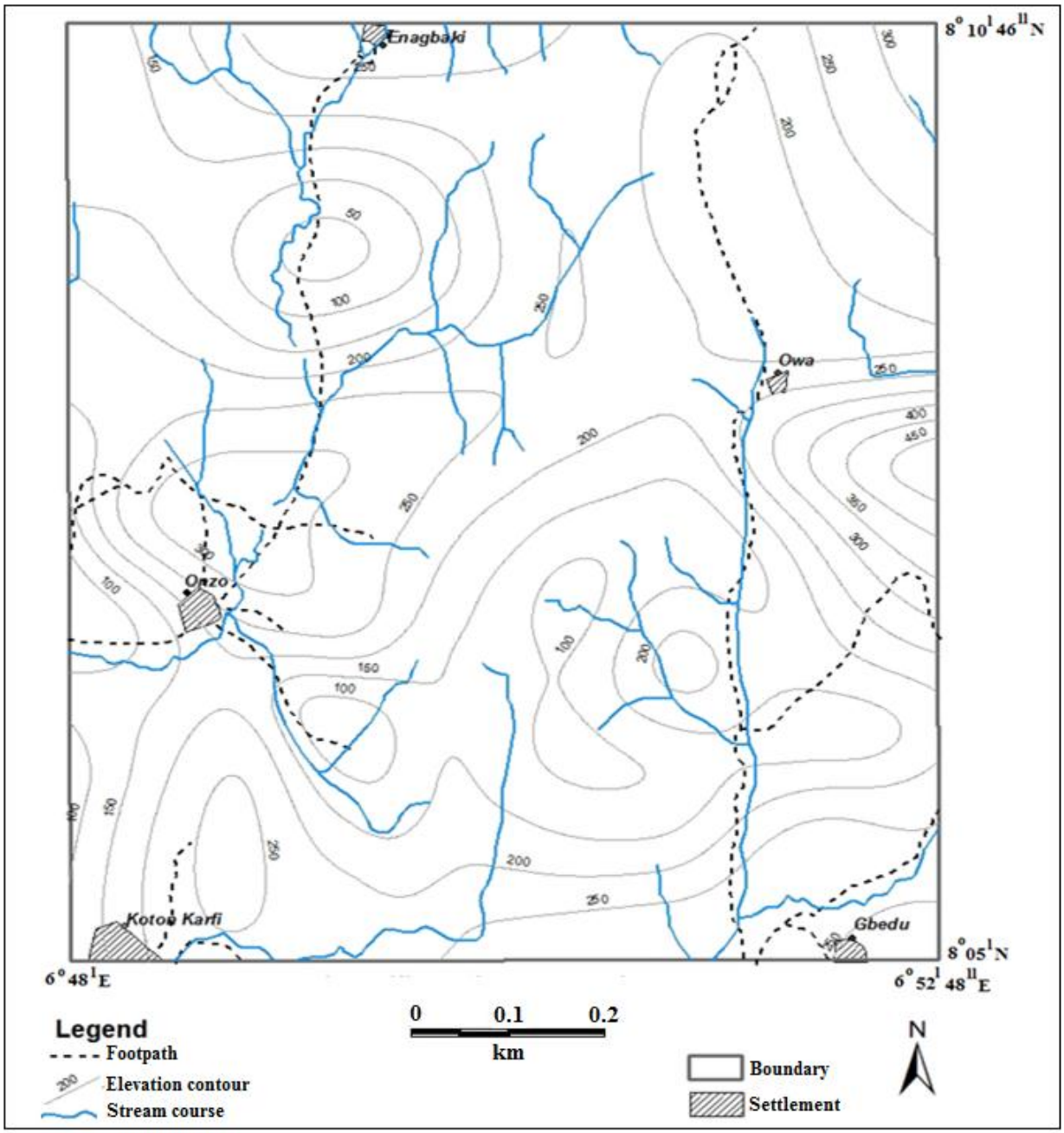

Fig. 2: Location map of the study area (Adapted from topographic map of sheet 227 Koton Karfi S.E., 1964)

2.0 MATERIALS AND METHODS

2.1 Sampling

Prior to field work, a base map of the area on a scale of 1:10,000 was prepared. Motor bikes, a global positioning system (GPS) device, compass-clinometer, M530 Kodak digital camera, hand lens, geological hammers, sample bags, permanent markers, masking tapes, pencils, field notebooks, tape-rule and field guides were employed to carry out the field mapping exercise.

The survey area was randomly traversed and rock samples at about 21 locations were identified and described, Table 1. Detail observation of the various rock types encountered on the field were made and recorded. The rock

types and locations were indicated on the base map with the aid of pencil and protractor. Various structural features that characterized the rock types were measured using the compass and the values recorded in the field notebook. Textural characteristics of the rocks were elucidated using magnifying glass. Rock samples of concretionary ironstone (Plate 1) and oolitic ironstone (Plates 2 and 3) were collected from the survey area. Samples were also obtained from a mining pit, about 5 m deep (Plate 4).

Plate 1 Dark brown concretionary ironstone (Latitude: 8.123˚ N, Longitude: 6.879˚ E)

Plate 2 Oolitic ironstone (Latitude: 8.158˚ N, Longitude: 6.849˚ E)

Plate 3 Oolitic ironstone (Latitude: 8.151˚N, Longitude: 6.821˚E)

Plate 4 Ironstone mining pit (Latitude: 8.158˚N, Longitude: 6.500˚E)

Table 1 Sample locations and their respective longitude and latitude coordinates

S/N	Sample Identification	Longitude {Decimal Degree}	Latitude {Decimal Degree}	Remark
1	Location 1	6.825	8.158	Brownish concretionary ironstone (obtained from mining pit)
2	Location 2	6.849	8.157	Brownish concretionary ironstone
3	Location 3	6.850	8.156	Weathered and loose brownish ironstone
4	Location 4	6.850	8.149	Small pebbles of brownish ironstones
5	Location 5	6.855	8.151	Fresh pebbles of ironstones, depleted and weathered
6	Location 6	6.855	8.159	Weathered, flat ironstone terrain, reddish brown in colour
7	Location 7	6.857	8.158	Brownish concretionary ironstone
8	Location 8	6.860	8.157	Brownish concretionary ironstone
9	Location 9	6.860	8.156	Slightly weathered ironstones with grassy vegetation
10	Location 10	6.849	8.158	Brownish concretionary ironstone
11	Location 11	6.838	8.158	Brownish concretionary ironstone
12	Location 12	6.842	8.152	Brownish concretionary ironstone
13	Location 13	6.846	8.138	Brownish concretionary ironstone
14	Location 14	6.821	8.151	Massive ironstone, relatively fresh exposed surface
15	Location 15	6.814	8.121	Brownish concretionary ironstone
16	Location 16	6.805	8.144	Brownish concretionary ironstone
17	Location 17	6.847	8.099	Brownish concretionary ironstone
18	Location 18	6.867	8.105	Dark brownish Oolitic ironstone, sample collected along water channel
19	Location 19	6.873	8.106	Dark brownish Oolitic ironstone
20	Location 20	6.849	8.158	Dark brownish Oolitic ironstone
21	Location 21	6.879	8.123	Brownish concretionary ironstone

2.2 Methodology of Samples Analysis

2.2.1 X-Ray Fluorescence Spectrometric Analysis

This exercise was carried out at the National Geoscience Research Labouratory Centre, Kaduna, Nigeria. Ironstone samples were crushed and grind to pass 150 mesh sieves (British standard). The powdered sample was loaded in a sample cup of the MiniPal4 x-ray fluorescence spectrometer model. Sample cups were identified with position numbers. The sample cup containing the powdered content was placed in a sample holder of the machine at a specific position, with position numbers ranging from 1–12. On selection of the specified position number; the spectrometer will rotate and bring the cup under x–ray focus. The x–ray bombards the sample and gives the result. The principle of measurement used is the Bragg's Law given by Bragg (1913):

$$n\lambda = 2d \sin \theta \quad (1)$$

where,

n = whole number

λ = wavelength of the element

d = spacing between successive planes of atoms

θ = compliment of the optical angle of incidence and reflection, that is 90^0 minus the angle of incidence.

2.2.2 Thin Section Analysis

A thin slice from a specimen was cut using diamond saw. One side of the specimen was polished to a perfectly smooth, flat surface and attached to a thin glass slide of about 0.03 mm thickness. The optical properties of minerals including those determined in plane – polarized light (PPL) and cross – polarized light (XP) were examined using the petrographic microscope.

2.2.3 Polished Section Analysis

A rock specimen was cut with a saw to obtain a slice. The slice was mounted on a glass. The two surfaces of the rock sample were grinded flat using carborundum powder and water; the sample surfaces were polished using an oily lubricant. Thus, the specimen under examination was prepared as a polished section on both sides. The optical properties of minerals including those determined in plane – polarized light and cross – polarized light were examined using the petrographic microscope.

3.0 RESULTS

3.1 Geology of the Study Area

The geological map of the study area is shown in Figure 3 on a scale of 1:10,000. The linearment information on Figure 4 is extracted from data modified after the structural map of Nigeria, 2007, scale 1:50,000; and confirmed with ground truthing. Lineaments (fractures) were observed in the survey area trending in the northwest–southeast (NW–SE), northeast–southwest(NE–SW), north–south(N–S) and east–west(E–W) directions.The NW–SE fracture system has fewer and shorter fractures truncated by the predominant NE–SW fractures in a pependicular direction. Stream channels shown in Figure 4 flow mainly in the NW–SE and NE–SW directions indicating that the drainage pattern is structurally controlled.

Figure 3 shows a bedding plane around location 9, at the east central section of the map striking in the northwest-southeast direction and dipping at 14^{o}. At the southern section of the map around location 17, two bedding planes are observed striking in the northwest-southeast direction and dipping at12^{o} and 13^{o} respectively. At the western section of the map around location 15, a bedding plane is observed striking in the northwest–southeast direction, dipping at 12^{o}. At the central section of the map around location 13, a bedding plane is observed striking in the northwest–southeast direction, dipping at 15^{o}. The succession of stratigraphic units within the survey area is described thus: ferruginized mudstones of the Agbaja

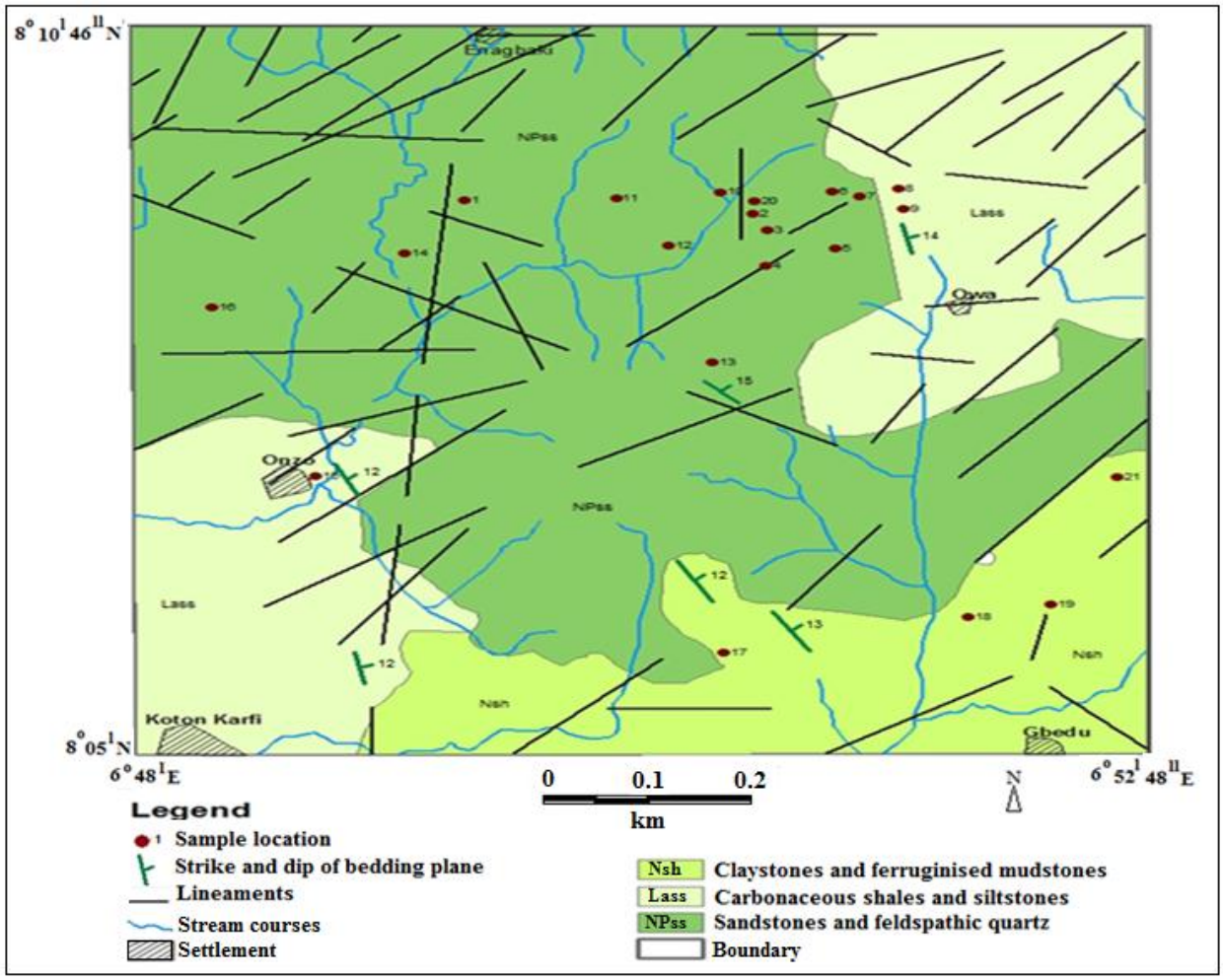

Fig. 3 Geological map of the study area

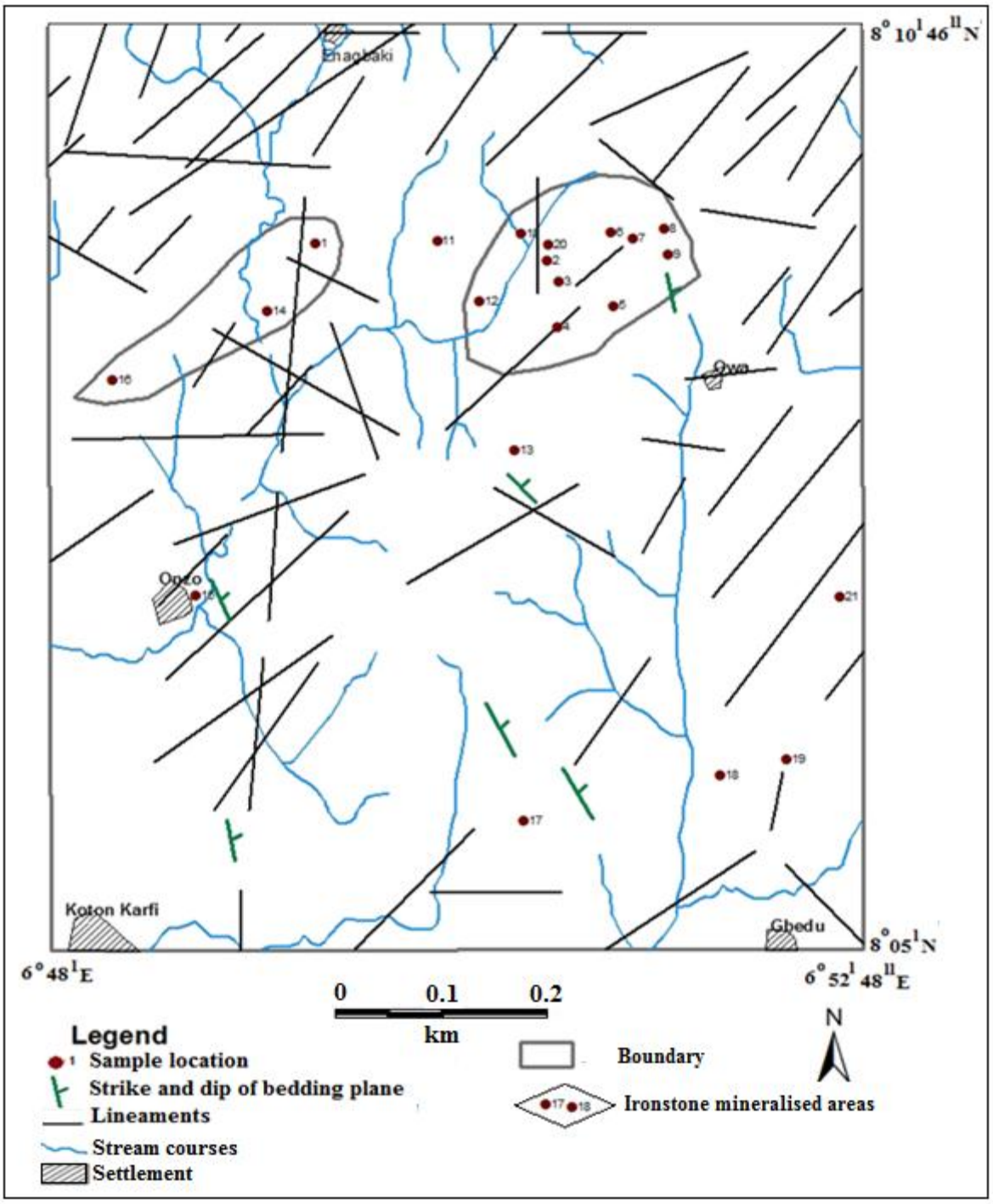

Fig. 4: Structural geology and ironstone mineralization map of the study area

Formation (NPss) overlying the sandstones, claystones and shales of the Patti Formation (Lass) which overlies the feldspathic sandstones and siltstones of the Lokoja Formation (Nsh). The Agbaja and Patti Formations are Maastrichtian in age; the Lokoja Formation is Campanian in age, Olabode, 2016. This stratigraphic succession is inferred from lithologic units observed from dried up stream channels and road cuttings within the study area. Figure 4 shows a northeast-southwest trending fabric of ironstone mineralised sections in the study area, suggesting a structurally controlled ironstone mineralization.

3.2 Geochemical Analysis

The concentration of Al_2O_3 ranges from 0.38% to 17.00%, with an average value of 8.49%. SiO_2 concentration ranges from 1.06% to 8.80%, with an average value of 4.32%. Fe_2O_3 content ranges from 74.00% to 94.04%, with an average value of 83.52%. Concentration of P_2O_5 ranges from 1.00% to 3.50% with an average value of about 2.32%. MnO content ranges from 0.08% to 8.44% with an average value of about 0.764% (Table 2). K_2O, Cr_2O_3, NiO_2, ZnO, La_2O_3, SrO, CuO, Nd_2O_3, Re_2O_7 and PbO generally have concentration less than 0.10%. Table 3 shows the composition of the later mentioned set of oxides expressed in parts per million (ppm).

3.3 Rhodonite and Wollastonite formation associated with ferruginization

Fe_2O_3—Al_2O_3—SiO_2 ternary map is shown in Figure 5 suggesting that unferruginization tends towards formation of alumina in the B—horizon, Zamanian *et al*., 2015. The brown corner is made up of silica. Various mineralization associated with the Fe_2O_3—Al_2O_3—SiO_2 ternary model is shown in Figure 6. Levels of laterization are illustrated in Figure 7. In the B—horizon, if Fe is being substituted by Mn, the mineral rhodonite ($MnSiO_3$), would be formed, Figure 8 ;(Johnson *et al*., 2005, Wilkinson and Humphreys, 2005). MnO is often nonstoichiometric, (Zamanian *et al*., 2015).

$MnO + SiO_2 \rightarrow MnSiO_3$

Fe_2O_3—CaO—SiO_2 ternary map is shown in Figure 9. CaO (calcia) minerals are very susceptible to weathering and leaching thereby leaving behind iron and alumina which are more resistive to weathering and leaching to form iron-related minerals such as hematite and goethite. Hence, increase in ferruginization and calsilicate content tends towards formation of wollastonite ($CaSiO_3$) in the B—horizon (Wilkinson and Humphreys, 2005).

Table 2 Composition of oxide constituents of ironstones displayed in weight percentage (wt %)

S/N	Sample ID	Lon. {Dec. Deg)	Lon. {Dec. Deg)	Al_2O_3	SiO_2	P_2O_5	CaO	V_2O_5	Eu_2O_3	MnO	Fe_2O_3	BaO
1	Loc 1	6.500	8.158	17.00	3.50	3.40	0.27	0.110	0.37	0.848	74.66	0
2	Loc 2	6.849	8.157	10.00	6.00	3.10	0.30	0.096	0.16	0.210	79.44	0
3	Loc 3	6.850	8.156	10.50	2.50	2.60	0.42	0.100	0	1.120	82.75	0
4	Loc 4	6.501	8.149	5.00	5.60	2.31	0.24	0.078	0	0.130	85.50	0
5	Loc 5	6.855	8.151	9.50	1.40	1.00	0.38	0.120	0.25	0.410	86.58	0
6	Loc 6	6.855	8.159	15.00	8.00	2.00	0.33	0.120	0.18	0.270	74.00	0
7	Loc 7	6.857	8.158	5.00	1.06	1.40	0.20	0.100	0.11	0.130	86.82	0
8	Loc 8	6.860	8.157	8.00	8.30	2.40	0.38	0.090	0.25	0.500	78.28	0
9	Loc 9	6.860	8.156	7.00	6.80	1.84	0.21	0.094	0.11	0.150	83.38	0
10	Loc 10	6.849	8.158	9.40	2.80	2.20	0.24	0.100	0.12	0.160	85.21	0
11	Loc 11	6.838	8.158	0.38	1.40	2.10	0.38	0.160	0.02	0.130	94.04	0
12	Loc 12	6.842	8.152	7.00	6.00	2.10	0.33	0.081	0.09	0.140	84.47	0
13	Loc 13	6.846	8.138	11.30	6.20	2.80	0.31	0.077	0.14	0.140	79.03	0
14	Loc 14	6.821	8.151	9.00	5.00	1.98	0.44	0.080	0	0.140	82.56	0
15	Loc 15	6.814	8.121	9.00	5.70	2.50	0.27	0.094	0.17	0.210	82.32	0
16	Loc 16	6.805	8.144	8.60	1.64	2.20	0.20	0.090	0.12	0.210	86.43	0
17	Loc 17	6.847	8.099	4.10	1.58	0	0.18	0.100	0.17	0.180	93.40	0
18	Loc 18	6.867	8.105	0	4.50	2.10	0.23	0.120	0.12	0.190	92.65	0
19	Loc 19	6.873	8.106	10.00	8.80	2.41	0.25	0.070	0.47	2.250	75.79	0
20	Loc 20	6.849	8.158	5.00	1.62	3.50	0.73	0.073	0	0.079	89.26	0
21	Loc 21	6.879	8.123	9.00	2.30	2.40	0.65	0.100	0	8.440	77.24	0.86
			Average	8.49	4.32	2.32	0.33	0.098	0.18	0.760	83.51	0.04

$CaO + SiO_2 \rightarrow CaSiO_3$

3.4 Differential accumulation of iron and manganese in relation to SiO_2/Al_2O_3 ratio

According to Furukawa *et al*. 1976, the differential concentration of either iron or manganese in ironstones as expressed by a ratio (termed iron-manganese ratio), $Fe_2O_3/ (Fe_2O_3+MnO)$ is positively correlated with the ratio SiO_2/Al_2O_3, all contents expressed in percentages shown in

Table 3 Composition of oxide constituents of the ironstones displayed in parts per million (ppm)

S/N	Sample ID	Lon. {Dec. Deg}	Lon. {Dec. Deg}	K_2O (ppm)	Cr_2O_3 (ppm)	NiO_2 (ppm)	ZnO (ppm)	La_2O_3 (ppm)	SrO (ppm)	CuO (ppm)	Nd_2O_3 (ppm)	Re_2O_7 (ppm)	PbO (ppm)
1	Loc 1	6.500	8.158	0	3400	0	840	300	850	380	0	300	0
2	Loc 2	6.849	8.157	0	100	0	430	700	0	40	90	200	0
3	Loc 3	6.850	8.156	0	0	0	810	500	730	0	0	400	0
4	Loc 4	6.501	8.149	0	350	60	500	600	0	200	0	300	0
5	Loc 5	6.855	8.151	0	300	0	460	400	1700	0	0	600	0
6	Loc 6	6.855	8.159	0	0	0	430	930	0	70	0	300	0
7	Loc 7	6.857	8.158	0	400	0	360	300	0	0	0	300	0
8	Loc 8	6.860	8.157	0	360	0	440	30	0	0	0	300	0
9	Loc 9	6.860	8.156	0	0	0	620	600	0	0	0	300	0
10	Loc 10	6.849	8.158	600	370	0	510	300	0	200	0	300	0
11	Loc 11	6.838	8.158	0	370	0	200	800	0	70	0	600	0
12	Loc 12	6.842	8.152	0	0	0	400	600	0	0	0	300	0
13	Loc 13	6.846	8.138	0	330	60	370	400	160	50	0	200	0
14	Loc 14	6.821	8.151	0	300	60	0	1000	0	50	0	300	0
15	Loc 15	6.814	8.121	0	330	300	410	200	0	30	0	300	0
16	Loc 16	6.805	8.144	0	330	0	530	300	0	50	0	300	0
17	Loc 17	6.847	8.099	0	200	10	520	500	60	20	0	300	0
18	Loc 18	6.867	8.105	0	0	0	490	300	0	110	0	300	0
19	Loc 19	6.873	8.106	0	320	30	730	0	0	0	0	300	0
20	Loc 20	6.849	8.158	0	340	0	810	0	0	20	0	300	0
21	Loc 21	6.879	8.123	1500	390	360	350	0	0	0	100	400	3500
			Average	100	530	130	510	490	700	100	100	300	170

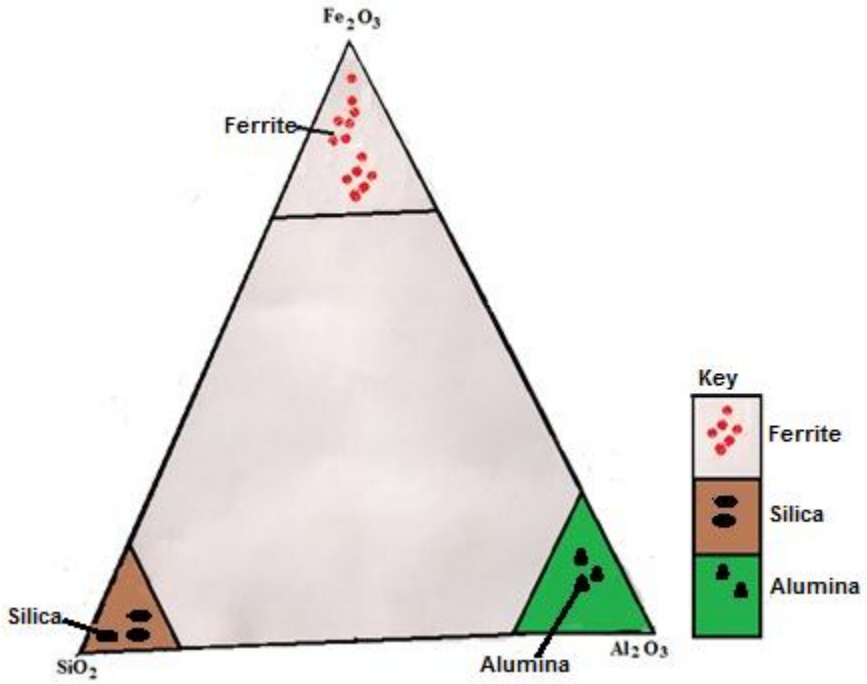

Fig. 5 Ternary map of wt. % (Fe_2O_3, Al_2O_3 and SiO_2) composition

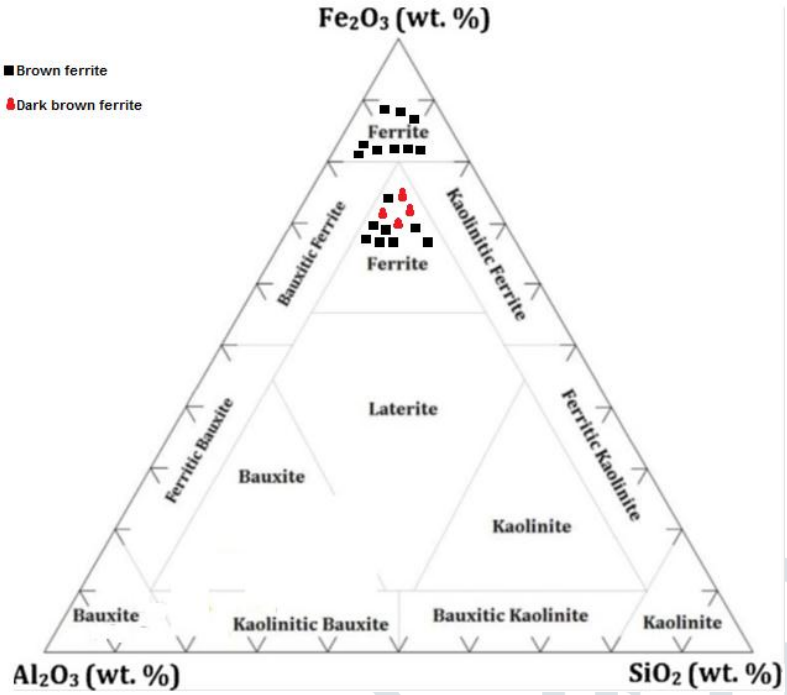

Fig.6 Triangular diagram of Fe_2O_3—Al_2O_3—SiO_2 (after Aleva, 1994) for ironstone ores

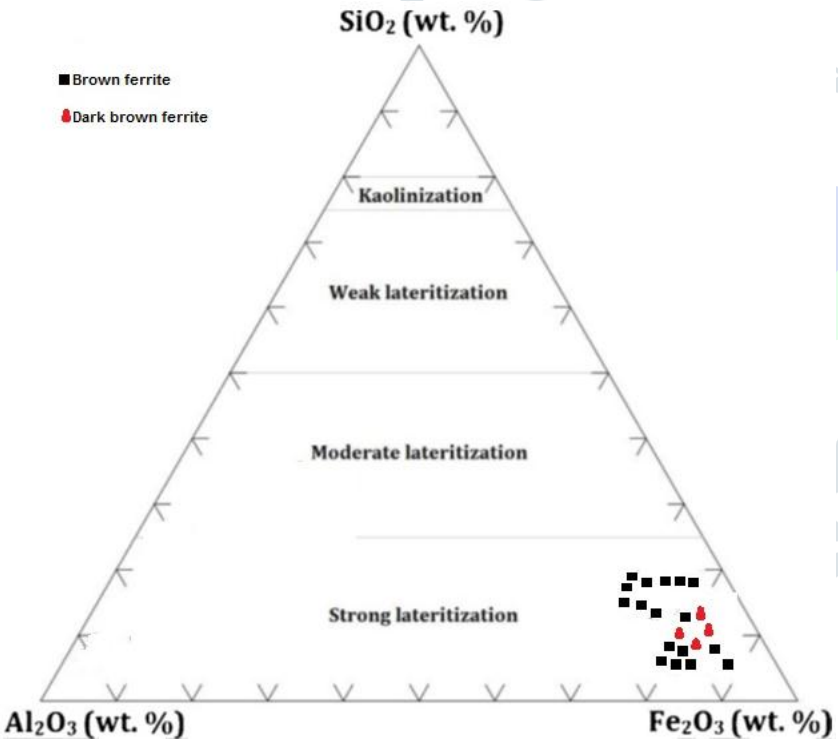

Fig. 7 Triangular diagram of Fe_2O_3—Al_2O_3—SiO_2 (after Shellmann, 1986) for ironstone ores, showing degree of laterization

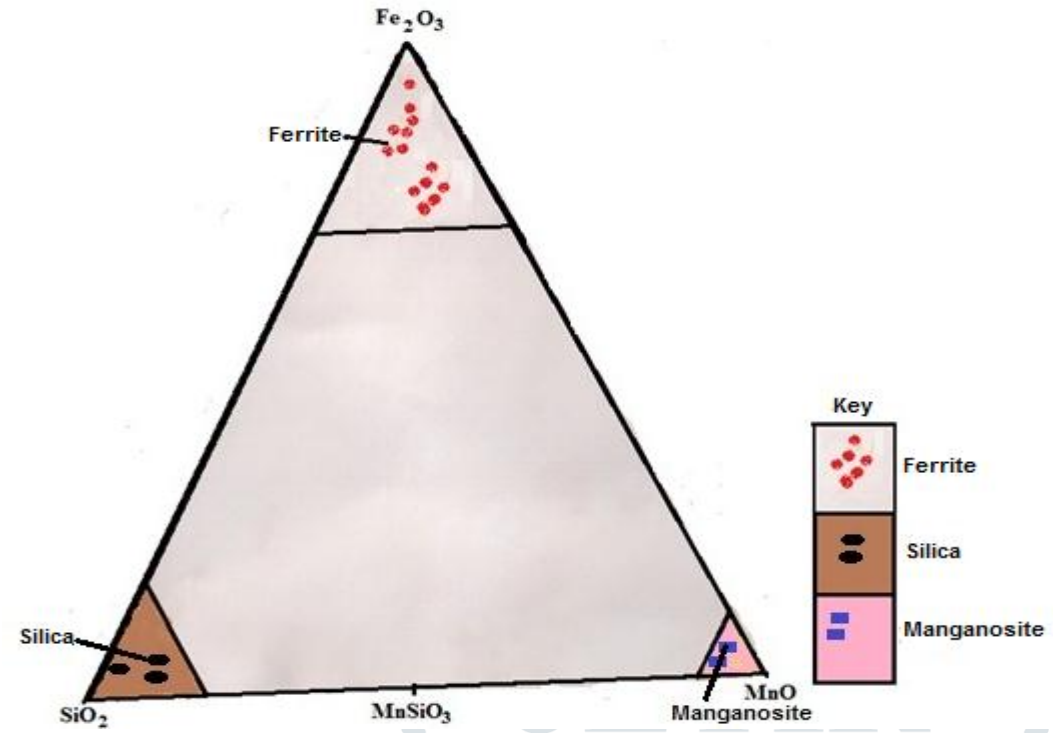

Fig. 8 Ternary map of wt. % (Fe_2O_3, MnO and SiO_2) composition

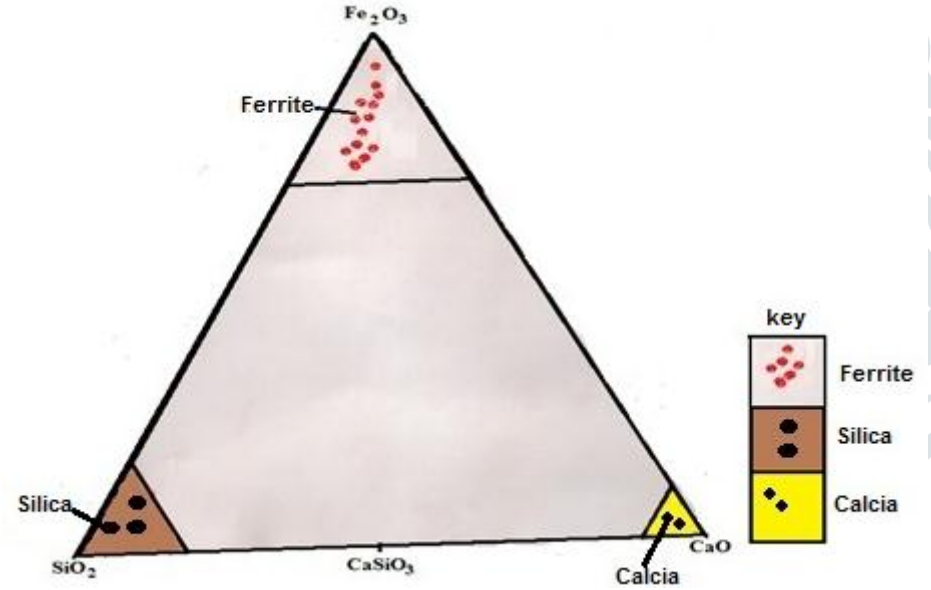

Fig. 9 Ternary map of wt. % (Fe_2O_3, CaO and SiO_2) composition

Table 4. The ratios are plotted on log−log coordinates shown in Figure 10. The positive correlation infers increase in iron relative to decrease in manganese content as the silica decreases

Table 4 Accumulation of Fe_2O_3 in relation to MnO, SiO_2 and Al_2O_3, after Furukawa *et al.* 1976

Sample ID	SiO_2/Al_2O_3 (A)	Fe_2O_3/ (Fe_2O_3+MnO) (B)	CaO+K_2O (C)	A/C	B/C	Log(A/C)	Log(B/C)
Loc 1	0.21	0.989	0.27	0.763	3.662	-0.118	0.564
Loc 2	0.60	0.997	0.30	2.000	3.325	0.301	0.522
Loc 3	0.24	0.987	0.42	0.567	2.349	-0.246	0.371
Loc 4	1.12	0.998	0.24	4.667	4.160	0.669	0.619
Loc 5	0.15	0.995	0.38	0.388	2.619	-0.411	0.418
Loc 6	0.53	0.996	0.33	1.616	3.019	0.208	0.480
Loc 7	0.21	0.999	0.20	1.060	4.993	0.025	0.698
Loc 8	1.04	0.994	0.38	2.730	2.615	0.436	0.417
Loc 9	0.97	0.998	0.21	4.626	4.753	0.665	0.677
Loc 10	0.30	0.998	0.30	0.993	3.327	-0.003	0.522
Loc 11	3.68	0.999	0.38	9.695	2.628	0.987	0.420
Loc 12	0.86	0.998	0.33	2.597	3.025	0.415	0.481
Loc 13	0.55	0.998	0.31	1.770	3.220	0.248	0.508
Loc 14	0.56	0.998	0.44	1.263	2.269	0.101	0.356
Loc 15	0.63	0.997	0.27	2.346	3.694	0.370	0.568
Loc 16	0.19	0.998	0.20	0.953	4.988	-0.021	0.698
Loc 17	0.39	0.998	0.18	2.141	5.545	0.331	0.744
Loc 18	0.00	0.998	0.23	0.000	4.339	0.000	0.637
Loc 19	0.88	0.971	0.25	3.520	3.885	0.547	0.589
Loc 20	0.32	0.999	0.73	0.444	1.369	-0.353	0.136
Loc 21	0.26	0.901	0.80	0.319	1.127	-0.496	0.052

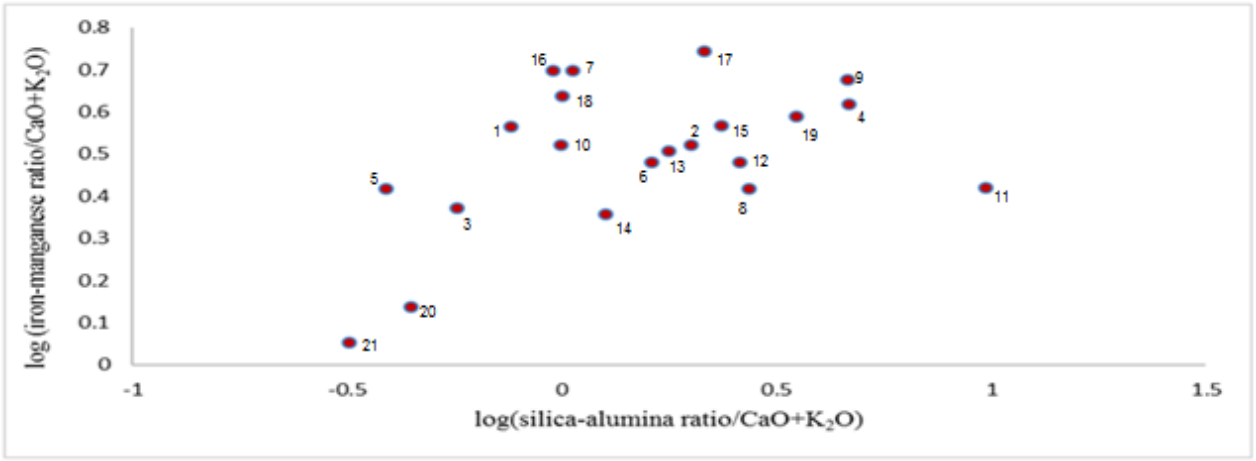

Fig. 10: Accumulation of Fe_2O_3 in relation to MnO, SiO_2 and Al_2O_3 (after Furukawa *et al.*, 1976)

relative to alumina. This result accords with the fact that iron oxides are relatively immobile compared to manganese oxides (Furukawa *et al.*, 1976).

3.5 Deleterious constituents of ironstones

The deleterious constituents of ironstones include P_2O_5, K_2O, Al_2O_3, SiO_2, S, ZnO and MnO. Figure 11 shows the deleterious constituents and their concentration at sampling points. Sulfur content is below detection limit in all the samples, probably due to iron enrichment in highly

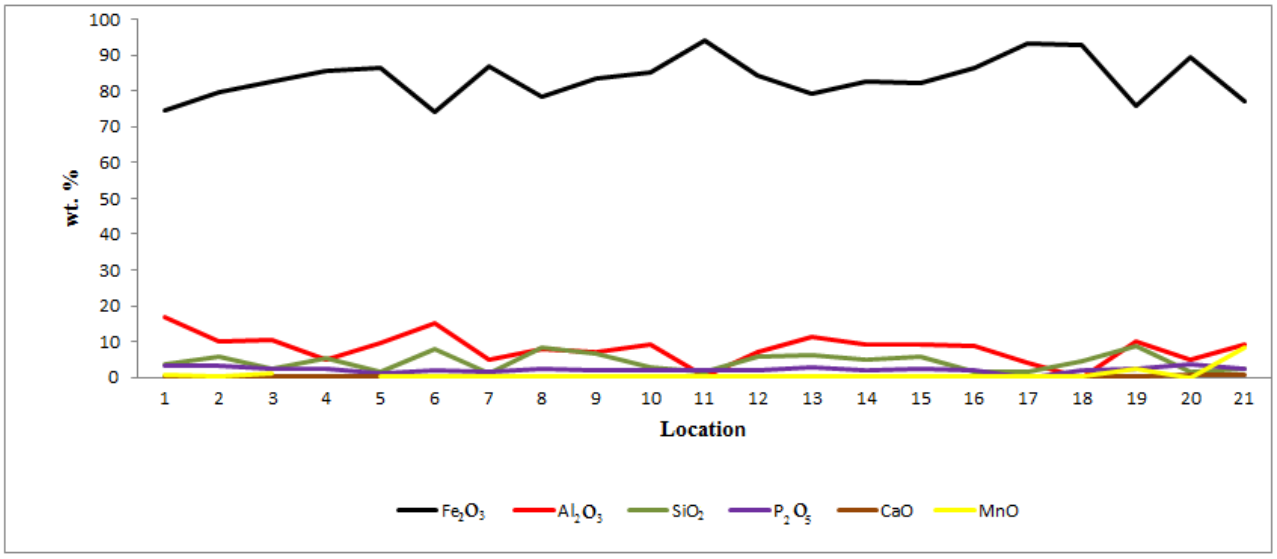

Fig. 11 Al_2O_3, SiO_2, P_2O_5 CaO, MnO and Fe_2O_3 concentration in ironstones at the sampling points

non–reducing environments. The diagram shows an increase in Fe_2O_3 content, and decrease in the concentration of Al_2O_3 from locations 1 to 3. At location 7, the concentration of Fe_2O_3 decreases to 77% while Al_2O_3 increases to 15.2 %. This trend continues up to location 21, indicating iron enrichment may be accompanied by depletion in alumina content probably due to weathering of rocks and replacement of elements during the ferruginization process. The sample at location 18 exhibited 92% Fe_2O_3 concentration and zero P_2O_5 content implying that iron enrichment may tend toward de-phosphorization.

Generally, every rise in Fe_2O_3 content is accompanied by a corresponding decrease in SiO_2 concentration and vice versa. This may imply that iron enrichment is accompanied by desilication probably due to weathering of rocks and replacement of elements during the ferruginization process. Desilication (or desilicification) is the removal of silicon from a soil horizon, relative to some less mobile component or components. Characteristic of pedogenesis in the tropics where silicon tends to be more mobile than iron and aluminum in well drained soils. The process is active in the formation of ferrallitic soils, laterites and bauxites, Zamanian *et al*., 2015.

3.6 Thin Section Petrographic Analysis

Petrographic studies were carried out on thin sections of specimens from locations (2, 5, 6, 7, 11, 17, 18 and 19). IM denotes iron oxide minerals and Q signifies quartz. Figure 12 (2, 5, 6, 7, 17, and 19) shows the ooidal pack-ironstone petrographic variety having radial structure with concentric laminations. The ooidal pack-ironstone is characterized by spherical, oblong and fragmented ooids. The ooids have nuclei with dark brown colour seen under plane polarized light or grey colour observed under cross polarized light. Peloids are also observed cemented by grains of ferruginous quartzite (Q) of the Itabirite type. Concentric laminae of goethite ooids may form several discrete zones of goethite suggesting iron enrichment zones, Figure 12{5}. Well sorted ooids and loosely parked ooids are shown in Figure 12{17 and 19}.

Figure 13{11 and 18} indicates detrital mud-ironstone petrographic variety, with brownish framboids of goethite after siderite, Figure 13{11} or fragmented brownish pseudomorphs of hematite after Itabirite, Figure 13{18}. Major mineral constituents include hematite and goethite. Quartz (Q) is also observed. The regular or irregular desiccation cracks are not mineralized.

3.7 Petrographic Analysis of Polished Sections

Polished slabs of detrital mud-ironstones are shown in Figure 14 (11, 18 and 20). Microscopic analyses of the ironstones reveal a botryoidal texture with brownish poorly sorted zones of hematite (IM) in Figure 14 (18 and 20). Ferruginous quartzite (Q) of the Itabirite type is also observed. The crystal system is trigonal. Bireflectance is weak with distinct anisotropy. Polishing hardness is less than pyrite.

Polished slabs of ooidal park-ironstones are shown in Figure 14 (2, 5 and 17). Petrographic analyses of the specimens reveal a botryoidal texture with angular grains of quartz (Q) and clusters of pseudomorphs of goethite after siderite (IM). Colour of the slab is bluish-grey while the crystal system is orthorhombic with a weak bireflectance. Polishing hardness is less than pyrite.

3.8 Modal Analysis of Ironstone Samples

Modal analysis of the thin sections, (Table 5) shows the ironstones having quartz mineral population less than 20%. The grains of quartz are angular in samples: Figure 12 (2, 5, 6, 7, 17 and 19) and Figure 13 (11 and 18); implying that they have not travelled far while the iron minerals acted as the cementing materials binding the grains together. The grains of quartz are rounded in Figure 12 {7}; signifying that they have travelled far while the iron minerals acted as the cementing materials binding the grains together.

Modal analysis of polished sections, (Table 6) shows the ironstones having quartz mineral population less than 20%. The grains of the quartz are angular and un-zoned in Figure 14 (2, 5, 11, 18 and 20); indicating that they have not travelled far while the iron minerals acted as the cementing materials binding the grains together.

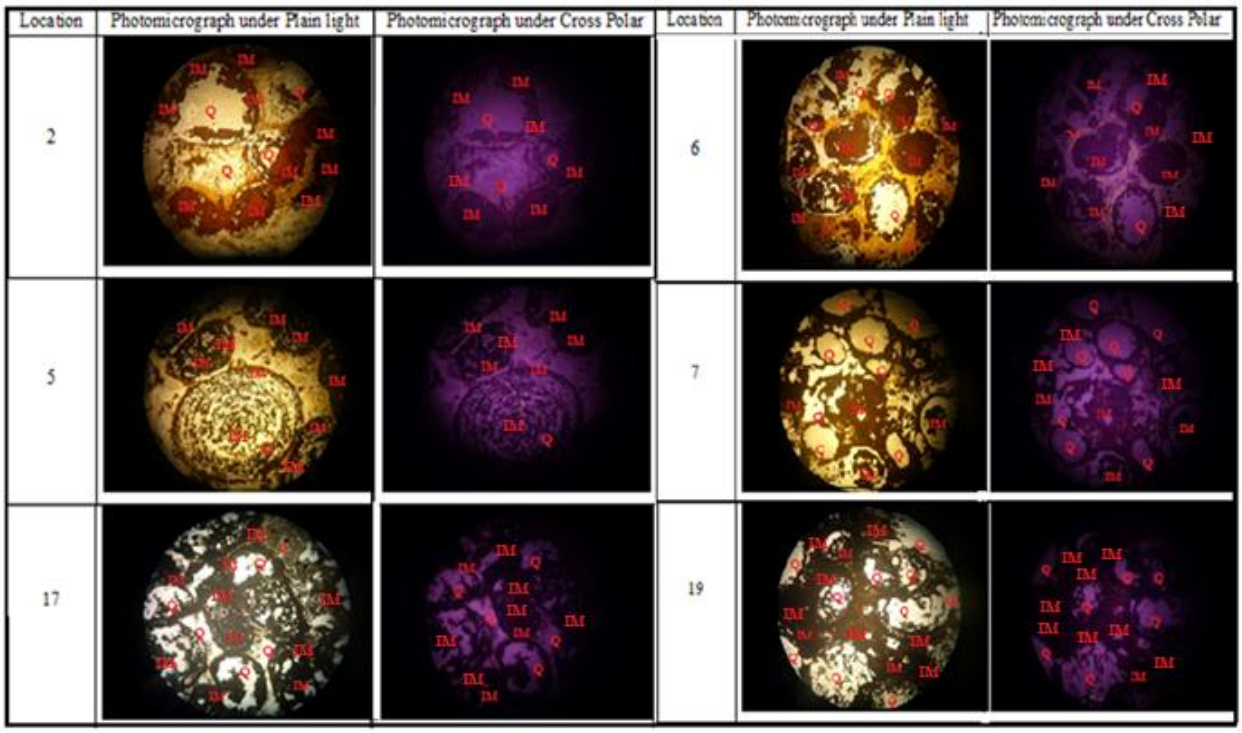

Fig. 12 Thin sections of ironstone samples from locations (2, 5, 6, 7, 17 and 19). IM = iron oxide minerals, Q=quartz, Magnification x 40

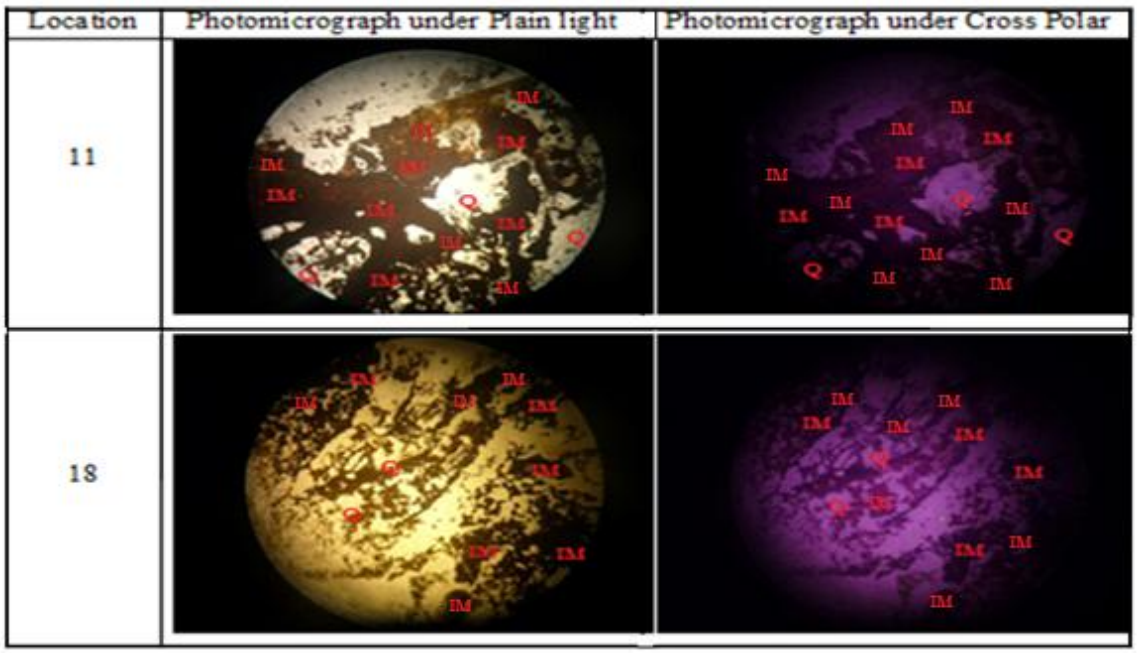

Fig. 13 Thin sections of ironstones samples from locations (11 and 18). IM = iron oxide minerals, Q=quartz, Magnification x 40

4.0 DISCUSSION AND CONCLUSION

4.1 Discussion

Drainage system of the study area is of the dendritic pattern and structurally controlled. The northwest-southeast fracture trend constitutes the conjugate trend to the northeast-southwest direction. The former trend is observed to be younger, being perpendicular, fewer and often truncate the northeast-southwest fracture system.

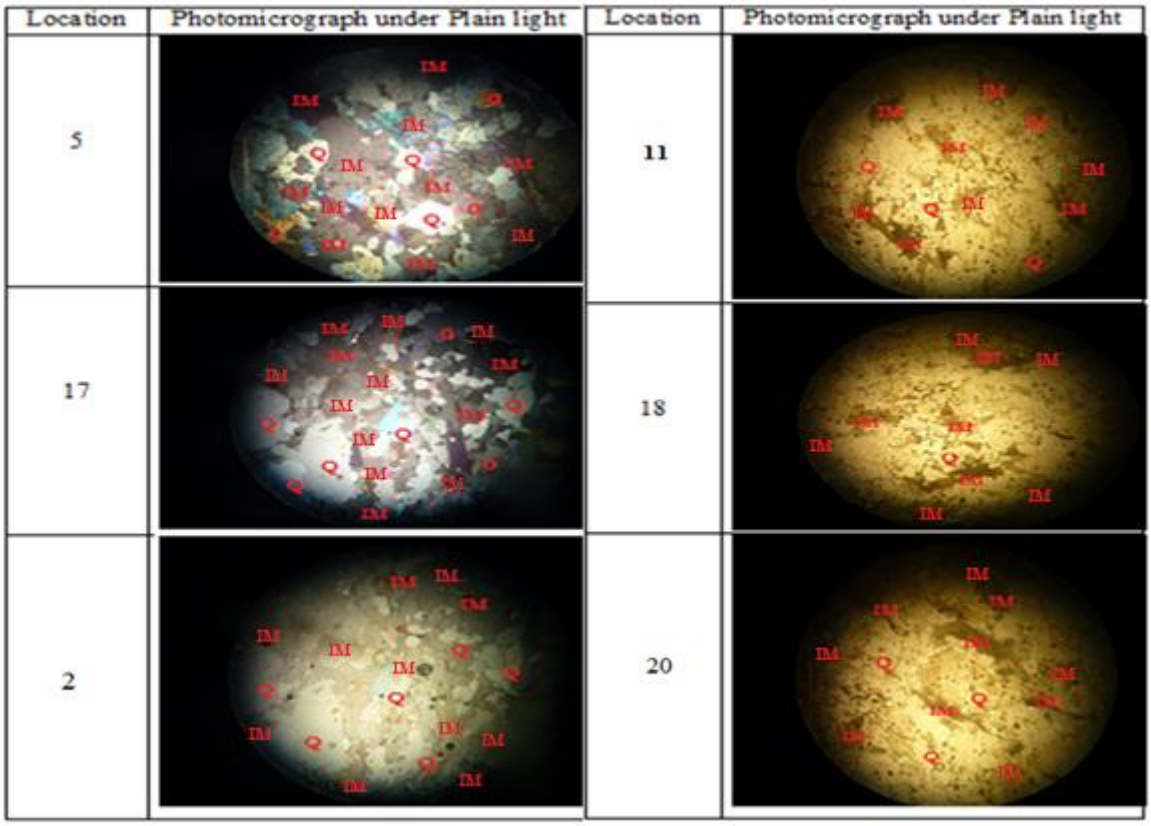

Fig. 14: Polished sections of ironstones samples from locations (2, 5, 11, 17, 18 and 20).IM=iron oxide minerals, Q=quartz or Quartzite, Magnification x 40

Table 5 Modal analysis in (%) for ironstone thin sections

Minerals	Modal analysis (%) for slide (Loc 2)	Modal analysis (%) for slide (Loc 5)	Modal analysis (%) for slide (Loc 6)	Modal analysis (%) for slide (Loc 7)	Modal analysis (%) for slide (Loc11)	Modal analysis (%) for slide (Loc 17)	Modal analysis (%) for slide (Loc 18)	Modal analysis (%) for slide (Loc 19)
Fe II oxides (Fe_2O_3)	70	70	60	65	75	75	75	65
Quartz	10	10	15	15	10	10	10	14
Others	20	20	25	20	15	15	15	21
Total	100	100	100	100	100	100	100	100

Table 6 Modal analysis in (%) for ironstone polished sections

Minerals	Modal analysis (%) for slide (Loc 5)	Modal analysis (%) for slide (Loc 17)	Modal analysis (%) for slide (Loc 11)	Modal analysis (%) for slide (Loc 2)	Modal analysis (%) for slide (Loc18)	Modal analysis (%) for slide (Loc 19)
Fe II oxides (Fe_2O_3)	65	55	60	70	80	70
Quartz	10	20	20	15	10	15
Others	25	25	20	15	10	15
Total	100	100	100	100	100	100

The study area comprises fine to coarse grained well sorted ferruginous sandstones, mud-stones, quartz, feldspar, and siltstones of the Patti Formation intercalated with sandstone facies. The ironstone Formation comprises two units namely pack-ironstone and mud-ironstone. Two petrographic varieties were identified viz: the ooidal pack-ironstone and detrital mud-ironstone. Spherical, oblong and fragmented ooids of pack-ironstone have complex mineralogy described by their cortex and nuclei. Minerals of the ooids are goethite, hematite and ferruginous quartzite of the Itabirite type. The core of the ooids is also made up of pseudomorphs of goethite after siderite or pseudomorphs of hematite after siderite.

Enrichment of the ooids resulted in the formation of minerals such as hematite and goethite. Adv ancing replacement and infilling of open space are common iron enrichment mechanisms in the ironstones. Irregular cavities within the ironstone matrix exhibit botryoidal texture while those created in the ooids are sometimes filled with milky white phosphorus mineral bolivarite and quartz which occur as disseminations within the goethitic matrix and veins of pack-ironstone and detrital mud-ironstones.

4.2 Conclusion

Iron enrichment is accompanied by a corresponding depletion of Al_2O_3 and SiO_2, moderate to extreme reduction of CaO, K_2O, V_2O_5, Cr_2O_3, Eu_2O_3, NiO_2, MnO, ZnO, La_2O_3, SrO, BaO, CuO, Nd_2O_3, Re_2O_7, PbO and a significant gain in P_2O_5, probably due to weathering. The significant depletion of these oxides with increasing ferruginization can be inferred to be a supergene nature of the replacement process. The replacement process can be described as desilication and depletion of alumina plus iron enrichment.

The high Fe_2O_3 concentration, zero sulfur content and generally low MnO and K_2O concentration suggest the ironstones as having minimal deleterious constituents.

ACKNOWLEDGEMENT

All the glory belong to God. The authors are grateful for the invaluable support provided by the staff of Geology and Mining Department, Nasarawa State University, Keffi, Nigeria. The geochemical analysis by the staff of National Geoscience Research Labouratory Centre, Kaduna, Nigeria is highly appreciated.

REFERENCES

Abimbola, A. F. 1994. *Mineralogical and geochemical studies of Agbaja ironstone Formation Nupe Basin Central Nigeria*, Ph.D. Thesis, University of Ibadan.

Adeleye, D. R. 1973. Origin of ironstones, an example from Middle Niger Valley, Nigeria, *Jour. of Sed . Petrol*., 43, 709 – 727.

Aleva, G.J.J.1994. *Laterites: Concepts, Geology, Morphology and Chemistry.* International Soil Reference and Information Centre (ISRIC), Waganingen, The Netherlands, 169.

Balogun, O. Y. 2000. *Senior Secondary Atlas*. *2nd Edn*, Nigeria: Longman.

Bragg, W.L.1913. The diffraction of short electromagnetic waves by a crystal. *Proceedings of the Cambridge Philosophical Society*, 17, 43–57.

Chard, J. 1995. *Making Iron and Steel: The Historic Processes, 1700-1900* Ringwood, NJ: North Jersey Highlands Historical Society.

Du Preez, J. W. 1956. Origin, classification and distribution of laterites. *Proc African Confr. Ibadan (3rd)*, 223 – 234.

Furukawa, H., Handawella, J., Kyuma, K., & Kawaguchi, K. 1976. Chemical, mineralogical and micro morphological properties of glaebules in some tropical lowland soils. *Southeast Asian Studies*, 13 (3), 1–24.

Johnson, D.L., Domier, E.J. and Johnson, D.N. 2005. Reflections on the nature of soil and its biomantle. *Annals, Association of American Geographers*, 95 (1), 11–31.

Jones, H. A. 1955. *The occurrence of oolitic ironstones in Nigeria: Their origin, geological history and petrology*. Ph.D. Thesis, Oxford University, 232.

Jones, H. A. 1958. The oolitic ironstones of Agbaja Plateau, Kabba Province. *Records of the Geol. Sur. Nigeria*, 20 – 43.

Kogbe, C. A. 1978. Origin and composition of the ferruginous oolites and laterites of NW Nigeria. *Geol. Rundsch Band* 67, Hert 2, 662 – 674.

Ladipo, K. O., Akande, S. O. and Mucke, A. 1988. Depositional environments, ore microscopy and origin of the Agbaja oolitic ironstone: *Abstr. Vol. NMGS*, 15.

Ladipo, K. O., Akande, S. O. and Mucke, A. 1993. Genesis of oolitic ironstone from the Middle Niger sedimentary Basin: evidence from sediment logical ore microscopic and geochemical studies, *Jour. Min. Geol.*

Ministry of Mines and Steel Development. 2010. Iron ore exploration opportunities in Nigeria.

Mucke, A. 1993. Post – diagenetic ferruginization of sedimentary rocks (sandstones, oolitic ironstones, kaolins and bauxites) including a comparative study of the reddening of red Beds. In: Development of sed., *Diagenesis*, 4.

Mucke, A., Ogunbajo, M. I. and Shekwolo, P. D. 1994. The Phanerozoic ironstones of the Bida Basin, Nigeria: Their mineralogy and genesis, *Abstr. Vol., NMGS.*

Obaje, N. G. 2009. *Geology andMineral resources of Nigeria* London: Springer, 1-100.

Obaje, N. G., Musa, M. K., Odoma, A. N. and Hamza, H. 2011. The Bida Basin in north-central Nigeria: sedimentology and petroleum geology. *Journal of Petroleum and Gas Exploration Research,* 1(1), 001 – 013.

Oguntoyinbo, J. S. 1978. Reflection coefficient of natural vegetation crops and urban surfaces in Nigeria. *Quart. Jour. Royal Met. Soc.* 96, 430 – 441.

Olabode, S. O. 2016. Soft sediment deformation structures in the Maastrichtian Patti Formation, southern Bida Basin Nigeria: Implications for the assessment of endogenic triggers in the Maastrichtian sedimentary record, *Open Journal of Geology*, 6, 410–438.

Oresajo, M. O. 1979. *Petrology and Geochemistry of Bassan-Nge Ironstone,* M.Phil. Thesis, University of Ibadan, Nigeria.

Shellmann, W. 1986. *A new definition of laterite*. Mem. Geol. Surv. India. 120:1–7.

Tattam, C. M. 1943. A review of Nigerian stratigraphy. *Rep. Geol. Surv., Nigeria*

Wilkinson, M.T. and Humphreys, G.S. 2005. Exploring paedogenesis via nuclide-based soil production rates and OSL-based bioturbation rates, *Australian Journal of Soil Research*, 43, 767–779.

Zamanian, H., Ahmadnejad, F. and Zarasvandi, A. 2015. Mineralogical and geochemical investigations of the Mombi bauxite deposit, Zagros Mountain, Iran, *Chemieder Erde Geochemistry*, 1–25.